# Effect of swelling agent on pore properties of mesoporous carbonated hydroxyapatite

# Effect of swelling agent on pore properties of mesoporous carbonated hydroxyapatite

**Nur Farahiyah Mohammad[1*], Nadia Liyana Amiruddin[1], Siti Shuhadah Md Saleh[2], Mustafa Ali Azhar Taib[3] and Nashrul Fazli Mohd Nasir[1]**

[1] Biomedical Engineering Research Group (BERG), School of Mechatronic Engineering, Pauh Putra Campus, Universiti Malaysia Perlis, 02600 Arau, Perlis, Malaysia
[2] School of Materials Engineering, Universiti Malaysia Perlis, Jejawi, 02600 Arau, Perlis, Malaysia
[3] Advanced Technology Training Centre (ADTEC) Taiping, PT 15643, Kamunting Raya, Mukim Asam Kumbang, 34600 Kamunting, Perak, Malaysia

* farahiyah@unimap.edu.my

**Abstract**. Mesoporous carbonated hydroxyapatite (CHA) has been seen to be suitable as an adsorbent material due to the proven biocompatibility, bioactivity and chemical stability. However, obtaining the high surface area and desired pore size for mesoporous materials become the main challenge in producing good quality adsorbent materials. Thus, this study aims to investigate the effect of addition of swelling agents on pore properties of mesoporous CHA. Mesoporous CHA was synthesised by precipitation method. Triblock co-polymer, P123 surfactant was used as a soft template to introduce pores within the CHA particles and 1-dodecanethiol as a swelling agent. Two different mixing temperature (60℃ and 80℃) were used during the mixing process of P123-calcium solution and 1-dodecanethiol. The effect of different mixing temperature (60℃ and 80℃) and various concentration of swelling agent on the phase, morphology and pore characteristics of mesoporous CHA were investigated using various material characterization techniques. Mixing temperature 60ºC, produced mesoporous CHA with much higher surface area (92.8 $m^2/g$), larger pore size (22.9 nm) and higher pore volume (0.502 $cm^2/g$) than those produce at 80ºC (surface area = 62.7 $m^2/g$, pore size = 2.6 nm and pore volume = 0.105 $cm^2/g$). The highest surface area (146.9 $m^2/g$) of mesoporous CHA was obtained when there was no swelling agent added. However, the pore size of the sample was very small. Therefore, the optimum pore characteristics (surface area = 104.5 $m^2/g$, pore size = 24.4 nm and pore volume = 0.530 $cm^2/g$) of mesoporous CHA was obtained when the swelling agent concentration is 0.6 M and the mixing temperature is 60ºC. Both mixing temperature and swelling agent concentration have profound effect on the pore characteristics of mesoporous carbonated hydroxyapatite (CHA).

## 1. Introduction

Conventional haemodialysis machine mostly used cellulose membranes for filtration. However, the filtration process can only remove small molecular weight uremic toxins [1]. New materials such as

activated carbon [2-4], zeolites [5] and graphene oxide have been utilized to enhance the dialysis treatment. However, these material have some limitations such as the inability to filter out medium and large molecular weight [6]. Some of these materials even producing another uremic toxin such as methyl guanidine as reported when activated carbon is utilized as filter material [4]. Medium and large molecular weight uremic toxin for example *p-cresol* and *β2-microglobulin* could not pass through the membrane. As for the *p-cresol* assembled, the patients might face immune defect, inhibition of blood clot formation and increase cardiovascular mortality [7]. Basically, the inability to remove *p-cresol* will lead to intoxication. Meanwhile, the accumulation of *β2-microglobulin* inside human body will promote cancer progression. Thus, it is essential to ensure that a haemodialysis system is able to filter out these uremic toxins.

So, there is a need for a new material that able to adsorb large molecular weight uremic toxin. The material should have high surface area that will promote high adsorption capacity. Mesoporous CHA is defined as a nanoporous bioceramic which indicated the size of pore within 2 nm to 50 nm in diameter [1]. Mesoporous CHA previously has been proven to have high surface area up to 78 $m^2/g$ [8]. Mesoporous CHA microspheres also demonstrated higher drug loading efficiency of 70-75% with gentamicin [9]. Consequently, this has proved that mesoporous CHA is a capable adsorbent material. However, obtaining the high surface area and desired pore size for mesoporous materials become the main challenge in producing good quality adsorbent materials. Therefore, this study aimed to synthesize mesoporous CHA by precipitation method using swelling agent as pore characteristics controller and to investigate the effect of mixing temperature and concentration of swelling agent on pore characteristics of mesoporous CHA.

## 2. Methodology

### *2.1 Materials*

The chemicals used as the calcium and phosphate precursor were calcium nitrate tetrahydrate ($Ca(NO_3)_2.4H_2O$) and diammonium hydrogen phosphate ($(NH_4)_2.HPO_4$) respectively. Ammonium hydrogen carbonate ($NH_4HCO_3$) was used as a carbonate precursor. Non-ionic triblock co-polymer Pluronics® P123, ($PEO_{19}PPO_{69}$ $PEO_{19}$) donated by BASF, USA was used as the structure directing agent for the pore template. 1-Dodecanethiol ($C_{12}H_{26}S$) was used as swelling agent. Besides that, sodium hydroxide (NaOH) was used to maintained the pH of the mixtures at pH 11. Commercial hydroxyapatite (HA), obtained from Taihei Chemical Industries, Osaka, Japan was used as the control sample.

### *2.2 Sample preparation*

P123, a non-ionic surfactant was dissolved in 100 ml of distilled water, followed by the addition of 9.446 g Ca $(NO_3)_2.4H_2O$ to obtain the clear micellar solution. Then, 6.3 g of 1-dodecanethiol was added into the mixtures. The surfactant-calcium-swelling mixed solution was stirred at 60℃. In the meantime, 3.17 g of diammonium hydrogen phosphate and 1.897 g of ammonium hydrogen carbonate was dissolved in 60 ml distilled water in another beaker. The phosphate-carbonate mixture was dripped slowly into surfactant-calcium-swelling mixed solution under continuous stirring motion until a milky suspension was yielded. During the mixing process, pH of the mixture was maintained at pH 11 throughout the mixing process using sodium hydroxide (NaOH). The mixture was then aged for 24 hours at room temperature. Then, the resulted white precipitate was centrifuged and washed for five times. Next, the white precipitate was dried in an oven at 100 $^0$C for 24 hours and ground into fine powders using mortar and pestle. Finally, the as-synthesised white powders were calcined at 550℃ for 6 hours. The final product was name as CHA-60-6.3. The whole process was then repeated for 80℃ mixing temperature, which donated as CHA-80-6.3. Similarly, the process repeated by using different swelling agent concentrations and control sample (without swelling agent) which designated in this article as listed in Table 1.

**Table 1.** Samples denotation

| Sample | Concentration of swelling agent (Molarity) | Synthesize temperature (℃) |
|---|---|---|
| HA (control) | - | Room temperature |
| CHA | - | Room temperature |
| CHA-80-6.3 | 0.3 M | 80ºC |
| CHA-60-6.3 | 0.3 M | 60ºC |
| CHA-60-12.6 | 0.6 M | 60ºC |
| CHA-60-18.9 | 0.9 M | 60ºC |

*2.3 Characterization of sample*

Rikagu Ultima IV, X-ray Diffraction (XRD) diffractometer was used to identify the phase present in the sample. Meanwhile, Fourier Transform Infrared (FTIR) analysis was performed for the identification of functional group that represent the CHA sample in the range of wave numbers of 400 $cm^{-1}$ to 4000 $cm^{-1}$. Morphological surface of the sample was studied by Scanning Electron Microscope (SEM). Nitrogen adsorption-desorption isotherms were measured with a Micromeritrics TriStar. Brunauer-Emmett- Teller (BET) equation was used to measured specific surface area. Barrett-Joyner-Halenda (BJH) equations was used to calculate pore size distribution (PSD) of the samples.

## 3. Result and discussion

*3.1 Effect of swelling agent mixing temperature on mesoporous CHA*

The XRD patterns of the synthesized sample of mesoporous CHA with different swelling agent mixing temperature are shown in Figure 1. The XRD results show that the phase of synthesis powder is a pure phase of CHA with reference to PDF pattern 01-089-7834 (CHA). No characteristic peaks of intermediate phase are observed in the XRD patterns, indicating that the main inorganic phase of the sample is CHA. Three main characteristics peaks of CHA 2θ = 25.8º, 31.8º and 33.0º which are indexed at (002), (211) and (300), are clearly seen in all XRD patterns of CHA and HA samples. However, the characteristic diffraction peak (112) is present only in XRD spectrum of HA at 2θ = 32.2º. The absent of this peak on XRD patterns of CHA most probably due to the broadening of the peaks indicate that CHA has lower crystallinity than HA. Besides that, diffraction of (102) located at 2θ = 28.1º is disappear from the XRD analysis on sample of CHA-80-6.3 compared to the others CHA sample.

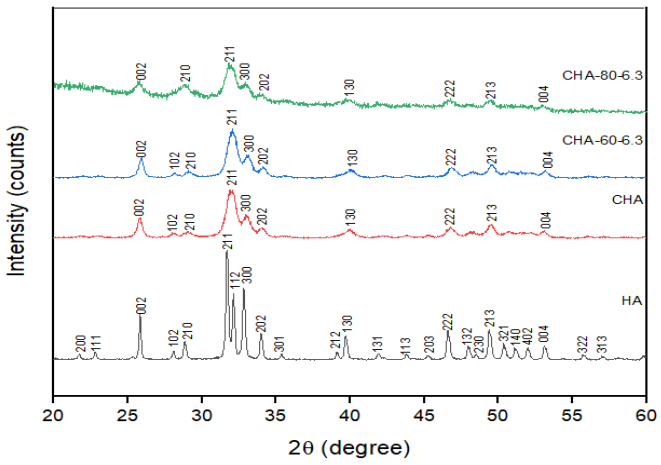


**Figure 1**. XRD patterns of samples synthesised using different mixing temperature

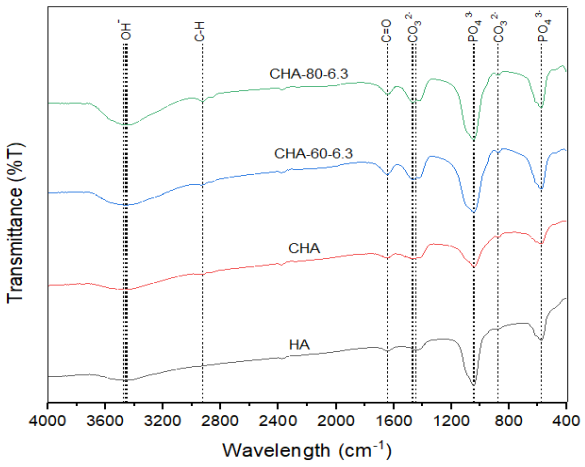


**Figure 2**. FTIR spectra band of the samples synthesised using different mixing temperature

The FTIR spectra of all samples are consistent (Figure 2) whereby the characteristic bands for mesoporous CHA are present in the samples. There are five functional groups presents in all mesoporous CHA samples. The bands appeared at wavelength = 3478.6 $cm^{-1}$, 3461.21 $cm^{-1}$, 3452.5 $cm^{-1}$ and 3465.18 $cm^{-1}$ are the characteristics for the $OH^-$ functional group. Meanwhile, the absorption peaks for $CO_3^{2-}$ functional group presents in two wavelength areas which are at 1450 $cm^{-1}$ to 1410 $cm^{-1}$ and 800 $cm^{-1}$ to 880 $cm^{-1}$. The absorption peaks at 1017 $cm^{-1}$, 962 $cm^{-1}$ and 567 $cm^{-1}$, 603 $cm^{-1}$ contributed to the stretching vibration ($V_3$) and vibration ($V_4$) for $PO_4^{3-}$ functional group respectively. Furthermore, C=O functional group appeared in the sample at wavelength ranging from 1640 $cm^{-1}$ to 1690 $cm^{-1}$. Lastly, at wavelength of 2850 $cm^{-1}$ to 3000 $cm^{-1}$ which is for C-H stretching band presents in the sample.

The morphology of mesoporous CHA and the HA was observed by SEM as shown in Figure 3. The SEM images revealed that the CHA powders are consists of very fine agglomerated particles, regardless of the mixing temperatures used. All the CHA particles are in irregular shape that formed fine agglomerates with some hollow spaces between them. Meanwhile, the HA particles demonstrated a rod-like structure that look like rice grains.

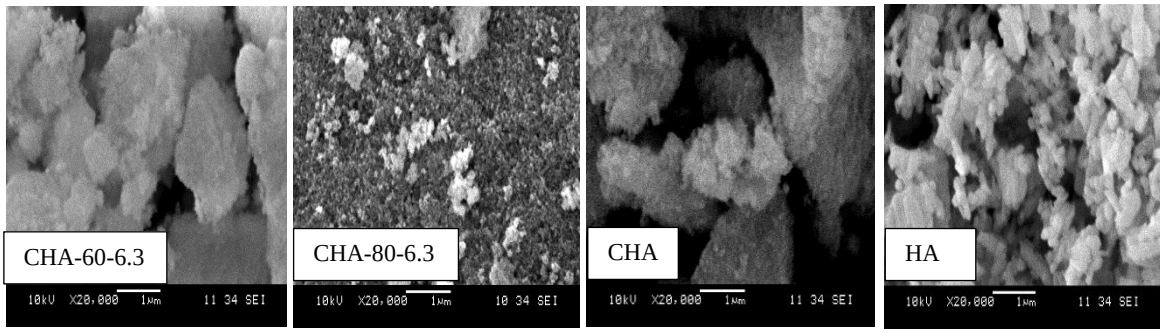


**Figure 3**. Morphological images of CHA samples synthesised with different swelling agent mixing temperature.

Figure 4 shows the nitrogen adsorption–desorption isotherms and the corresponding Barrett–Joyner–Halenda (BJH) pore size distribution. All mesoporous CHA samples exhibited type IV character with H1 hysteresis loop. An obvious step could be seen at P/Po= 0.8 – 1.0. The result obtained indicates that CHA-60-6.3 sample has the highest sorption properties among the samples followed by CHA, CHA-80-6.3 and HA. The isotherm curve of HA is identified as Type II isotherm, which is the common form isotherms of non-porous materials.

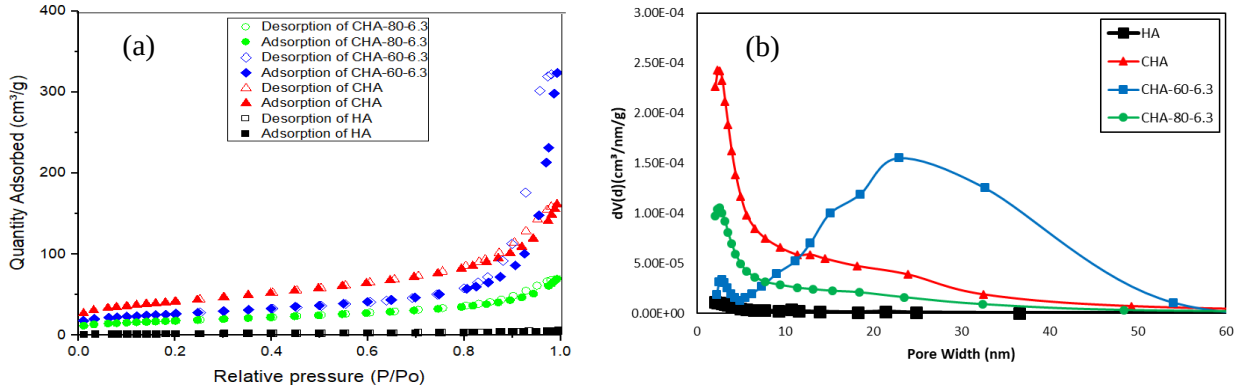


**Figure 4**. (a) Nitrogen adsorption–desorption isotherms and (b) pore size distribution of CHA-80-6.3, CHA-60-6.3, CHA and HA.

Table 2 presented the pore properties of mesoporous CHA samples with different synthesis temperature. The mesoporous CHA that synthesised without swelling agent have the highest BET surface area which is 146.9 $m^2/g$ compared to the other samples. However, the surface area decreased as the 1-dodecanethiol was added during the synthesis process as shown by the BET surface area of CHA-80-6.3 and CHA-60-6.3 (62.7 $m^2/g$ and 92.8 $m^2/g$). Lower mixing temperature produce mesoporous CHA with higher surface area, pore size and pore volume compared to higher mixing temperature. Increasing the synthesis temperature is expected to increase the pore properties of the sample since the hydrophobic molecule are expected to interact with the surfactant. However, in this study the increasing of mixing temperature could not promote bigger pore properties of the samples. As stated in previous studies, the interaction between these molecules could be enhanced by having other controllable parameters such as basic pH conditions and fixed amount of NaOH solution [10-12].

**Table 2**. The surface area, pore volume, pore size of mesoporous CHA samples

| Sample | BET surface area ($m^2/g$) | BJH pore size (nm) | BJH pore volume ($cm^3/g$) |
|---|---|---|---|
| HA | 7.8 | 2.0 | 0.008 |
| CHA | 146.9 | 2.3 | 0.244 |
| CHA-80-6.3 | 62.7 | 2.6 | 0.105 |
| CHA-60-6.3 | 92.8 | 22.9 | 0.502 |
| CHA-60-12.6 | 104.5 | 24.4 | 0.530 |
| CHA-60-18.9 | 108.6 | 22.9 | 0.525 |

### *3.2 Effect of swelling agent concentration on mesoporous CHA*

The samples prepared with different concentration of swelling agent were characterized using XRD. As shown in Figure 5, the XRD of CHA-60-6.3, CHA-60-12.6 and CHA-60-18.9 show diffraction peaks similar to CHA (PDF#01-089-7834), indicating that pure phase had successfully synthesised. No characteristic peaks of intermediate phase observed diffraction pattern indicating that the main inorganic phase of the sample is CHA. XRD pattern of CHA samples are compared to the HA in order to further confirmed the formation of pure CHA. Three main characteristic peaks of CHA at $2\theta = 25.8^o$, $31.8^o$ and $33.0^o$ which can be indexes at (002), (211) and (300), are clearly seen in all XRD patterns of CHA and HA samples. However, the characteristic diffraction peak (112) is present only in XRD spectrum of HA at $2\theta = 32.2^o$. The absent of the peak characteristic on XRD pattern of CHA samples most probably due to the broadening of the sample. Besides, the present of P123 surfactant during synthesis process might disturbed the long-range order of the crystal structure.

Furthermore, the FTIR spectroscopy of the CHA-60-6.3, CHA-60-12.6 and CHA-60-18.9 all was investigated (Figure 6). As shown in Figure 6, the bands appeared at wavelength = 3465.18 $cm^{-1}$, 3478.6 $cm^{-1}$, 3461.21 $cm^{-1}$ and 3457.33 $cm^{-1}$ are the characteristic band for the $OH^-$ functional group where $OH^-$ stretch presents at 3200 $cm^{-1}$ to 3500 $cm^{-1}$. Meanwhile, the absorption peaks for $CO_3^{2-}$ functional group presents at 1450 $cm^{-1}$ to 1410 $cm^{-1}$ and 800 $cm^{-1}$ to 880 $cm^{-1}$ where all samples have $CO_3^{2-}$ functional group as in Figure 6. The absorption peaks at 1017 $cm^{-1}$, 962 $cm^{-1}$ and 567 $cm^{-1}$, 603 $cm^{-1}$ are the stretching vibration ($V_3$) and vibration ($V_4$) for $PO_4^{3-}$ functional group respectively. Furthermore, there was also C=O functional group appeared in the sample at wavelength ranging from 1640 $cm^{-1}$ to 1690 $cm^{-1}$. Lastly, at wavelength of 2850 $cm^{-1}$ to 3000 $cm^{-1}$ which is for C-H stretching band presents in the sample. All functional groups appeared in the samples are compared from several reported works [10-16].

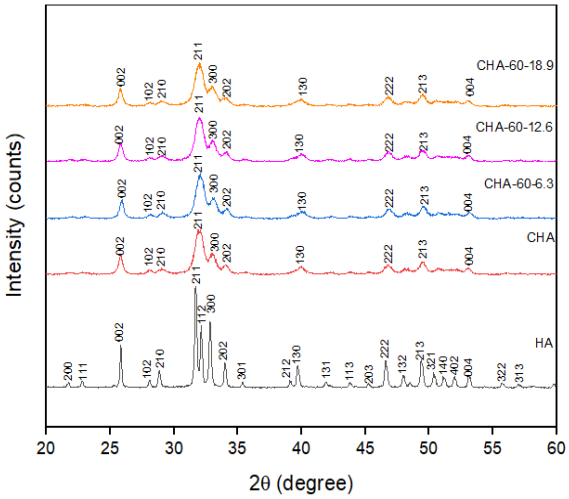


**Figure 5**. XRD patterns of samples synthesised using different swelling agent concentration

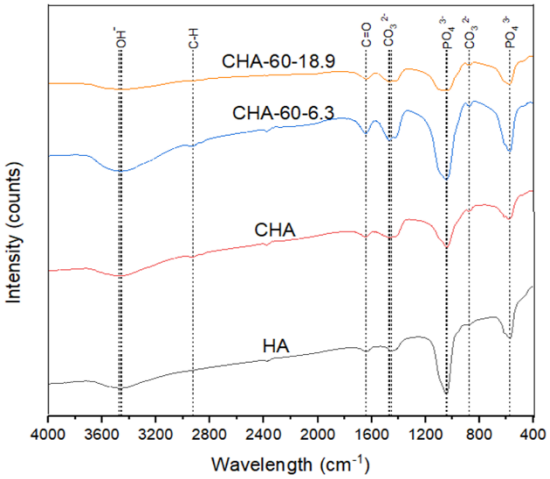


**Figure 6**. FTIR spectra band of the samples synthesised using swelling agent concentration

Figure 7 shows the morphological structure of HA, CHA, CHA-60-6.3 and CHA-60-18.9. Cylindrical particles are observed in the control HA sample while control CHA sample has an irregular shape. Close examination on the CHA sample showed the shapes were in transition process to a sphere shape micelle. Meanwhile, by adding swelling agent to the CHA samples, there is significant changes in the morphology of the samples. Samples synthesised with swelling agent has higher agglomeration compared to the control CHA sample. CHA particles become more agglomerated when concentration of swelling agent increase. The increment of the swelling agent concentration lead to the further diffusion of hydrophobic element of the swelling agent into hydrophobic section of the surfactant as stated in previous study[10]. Thus, the swelling process is occurred in the samples and foamy structured micelle could be obtained with further increment of swelling agent concentration.

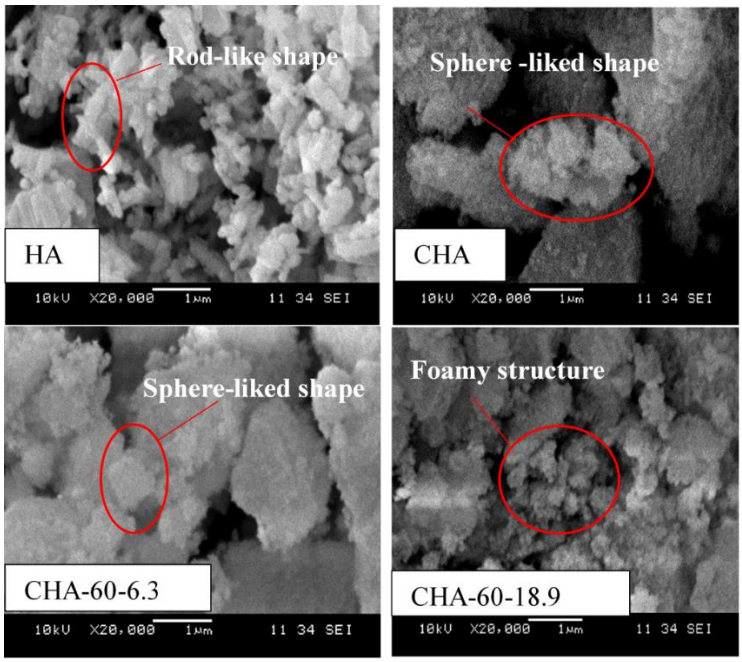


**Figure 7**. Morphological images of CHA samples synthesised with different swelling agent concentration

The nitrogen adsorption-desorption isotherm of CHA samples with different concentration of swelling agent are shown in Figure 8 (a). All CHA samples exhibited a Type IV character with H1 hysteresis loop where H1 hysteresis loop is associated with porous materials consists of agglomerates or compacts of approximately uniform spheres in a fairly regular array. It can obviously be seen that all CHA samples synthesized with swelling agent has higher distribution of adsorption-desorption properties when compared to CHA and HA sample. The result obtained indicates that CHA samples with swelling agent has the high sorption properties among the other sample. An obvious step could be seen at $P/P_o$= 0.8 – 1.0. The isotherm curve of HA is identified as Type II isotherm, which is the common form isotherms of non-porous materials. Figure 8(b) presented the corresponding BJH pore size distribution (PSD) graph for mesoporous CHA samples with different concentration of swelling agent. Basically CHA samples synthesised with swelling agent have similar pore size distribution pattern between 2.0 to 50 nm . The pore sizes for CHA-60-6.3 are mainly distributed at 22.9 nm, CHA-60-12.6 at 24.4 nm and CHA-60-18.9 at 22.9 nm. CHA are mainly distributed at 2.3 nm and HA are at 2.0 nm. CHA-60-12.6 has the highest peak, while HA sample has the lowest pore size distribution since it is non-porous material.

As shown in Table 2, BET surface area of the samples increase with the increase of concentration of swelling agent. BJH pore size and BJH pore volume increased when concentration of swelling agent is twice (0.6 M) of the initial concentration (0.3 M). Meawhile, the pore size and volume slightly decrease while the swelling agent concentration is three times (0.9 M) of the initial concentration. The introduction of swelling agent is expected to promote higher degree of swelling in the micelle structures. The hydrophobic molecules of the swelling agent will interact with surfactant molecules to initiate swelling process. Higher degree of pore expansion could be obtained by introducing more concentrated swelling agent. However, with further increase of the swelling agent from 0.6 M to 0.9 M, the pore size and pore volume suddenly decrease. This reduction might be due to the excessive amount of swelling agent introduced [10] into the mixture of the solution.

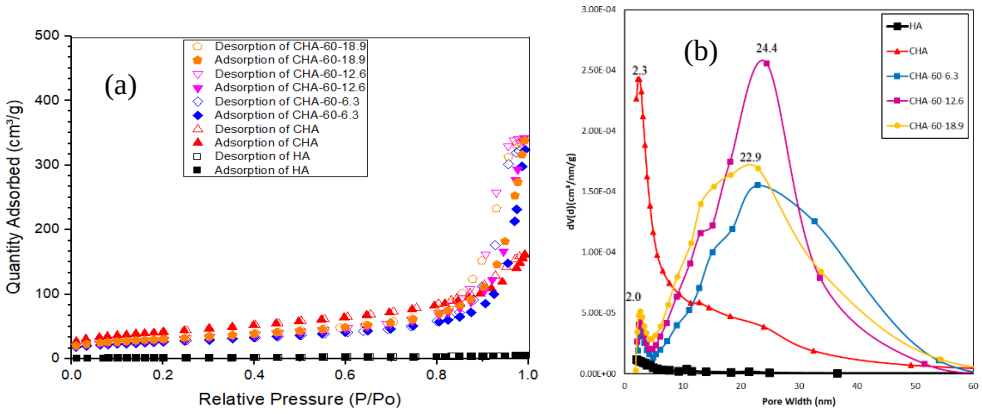


**Figure 8.** (a) Nitrogen adsorption–desorption isotherms and (b) pore size distribution of CHA-60-6.3, CHA-60-12.6, CHA-60-18.9, CHA and HA.

## 4. Conclusion

Mesoporous CHA samples have been successfully synthesized by chemical precipitation method. 1-dodecanethiol is utilized as swelling agent in order to study its effect on pore characteristics of mesoporous CHA sample. From the result obtained, swelling agent do affect the surface area and pore size of the mesoporous CHA sample. Introduction of swelling agent drastically reduced the surface area of mesoporous CHA. Therefore, to counter this drawback, 0.6 M of swelling agent should be mixed at 60°C to obtain much higher surface area (104 $m^2/g$) and pore size about 20-24 nm.

## 5. References

[1] Ooi C H 2014 Urea adsorption by activated carbon derived from oil palm kernel shell and empty fruit bunch fiber. (Penang: Universiti Sains Malaysia) p 157
[2] Krawczyk H 2009 Production of uremic toxin methylguanidine from creatinine via creatol on activated carbon *Journal of Pharmaceutical and Biomedical Analysis* **49** 945-9
[3] Mitome T, Uchida Y, Egashira Y, Hayashi K, Nishiura A and Nishiyama N 2013 Adsorption of indole on KOH-activated mesoporous carbon *Colloids and Surfaces A: Physicochemical and Engineering Aspects* **424** 89-95
[4] Howell C A, Sandeman S R, Zheng Y, Mikhalovsky S V, Nikolaev V G, Sakhno L A and Snezhkova E A 2016 New dextran coated activated carbons for medical use *CARBON* **97** 134-46
[5] Raharjo Y, Ismail A F, Othman M H D, Malek N A N N and Santoso D 2019 Preparation and characterization of imprinted zeolite-Y for p-cresol removal in haemodialysis *Materials Science and Engineering: C* **103** 109722
[6] Cheng Y-c, Fu C-c, Hsiao Y-s, Chien C-c and Juang R-s 2018 Clearance of low molecular-weight uremic toxins p -cresol , creatinine , and urea from simulated serum by adsorption *Journal of Molecular Liquids* **252** 203-10
[7] De Smet R, David F, Sandra P, Van Kaer J, Lesaffer G, Dhondt A, Lameire N and Vanholder R 1998 A sensitive HPLC method for the quantification of free and total p-cresol in patients with chronic renal failure *Clinica Chimica Acta* **278** 1-21
[8] Mohammad N F, Othman R, Abdullah A A and Yeoh F Y 2018 Effect of surfactant concentrations on pore characteristics of mesoporous carbonated hydroxyapatite prepared by soft-templating hydrothermal method *International Journal of Nanoelectronics and Materials* **11** 59-70
[9] Guo Y J, Long T, Chen W, Ning C Q, Zhu Z A and Guo Y P 2013 Bactericidal property and biocompatibility of gentamicin-loaded mesoporous carbonated hydroxyapatite microspheres *Materials Science and Engineering C* **33** 3583-91
[10] Bakhtiari L, Javadpour J, Rezaie H R, Erfan M and Shokrgozar M A 2015 The effect of swelling agent on the pore characteristics of mesoporous hydroxyapatite nanoparticles *Progress in Natural Science: Materials International* **25** 185-90
[11] Bakhtiari L, Rezaie H R, Javadpour J, Erfan M and Shokrgozar M A 2015 The effect of synthesis parameters on the geometry and dimensions of mesoporous hydroxyapatite nanoparticles in the presence of 1-dodecanethiol as a pore expander *Materials Science & Engineering C* **53** 1-6
[12] Bakhtiari L, Javadpour J, Rezaie H R, Erfan M, Mazinani B and Aminian A 2016 Pore size control in the synthesis of hydroxyapatite nanoparticles: The effect of pore expander content and the synthesis temperature *Ceramics International 42 (2016) 11259–11264*
[13] Ooi C H, Ling Y P, Pung S Y and Yeoh F Y 2019 Mesoporous hydroxyapatite derived from surfactant-templating system for p-Cresol adsorption: Physicochemical properties, formation process and adsorption performance *Powder Technology* **342** 725-34
[14] Mohammad N F, Othman R, Asma Abdullah N and Yee Yeoh F 2016 In vitro Evaluation of Mesoporous Carbonated Hydroxyapatite in MC3T3-E1 Osteoblast Cells *Procedia Chemistry* **19** 259-66
[15] Mohammad N F, Yeoh F-y and Othman R 2012 Synthesis & Characterization of Mesoporous Hydroxyapatite by Co- Synthesis & Characterization of Mesoporous Hydroxyapatite by Co-Precipitation Method
[16] Mohammad N F, Othman R and Yee Yeoh F 2015 Controlling the pore characteristics of mesoporous apatite materials_ Hydroxyapatite and carbonate apatite *Ceramics International 41 (2015) 10624–10633*